

PCCP

Accepted Manuscript



This is an *Accepted Manuscript*, which has been through the Royal Society of Chemistry peer review process and has been accepted for publication.

Accepted Manuscripts are published online shortly after acceptance, before technical editing, formatting and proof reading. Using this free service, authors can make their results available to the community, in citable form, before we publish the edited article. We will replace this *Accepted Manuscript* with the edited and formatted *Advance Article* as soon as it is available.

You can find more information about *Accepted Manuscripts* in the [Information for Authors](#).

Please note that technical editing may introduce minor changes to the text and/or graphics, which may alter content. The journal's standard [Terms & Conditions](#) and the [Ethical guidelines](#) still apply. In no event shall the Royal Society of Chemistry be held responsible for any errors or omissions in this *Accepted Manuscript* or any consequences arising from the use of any information it contains.

Cite this: DOI: 10.1039/xxxxxxxxxx

Simple analytical model for Signal Amplification by Reversible Exchange (SABRE) process

Danila A. Barskiy,^{*,a,‡} Andrey N. Pravdivtsev,^{*,a,b} Konstantin L. Ivanov,^{a,b}
Kirill V. Kovtunov,^{a,b} and Igor V. Koptyug^{a,b}

Received Date

Accepted Date

DOI: 10.1039/xxxxxxxxxx

www.rsc.org/journalname

We demonstrate an analytical model for the description of the Signal Amplification By Reversible Exchange (SABRE) process. The model relies on a combined analysis of chemical kinetics and evolution of the nuclear spin system during the hyperpolarization process. The presented model for the first time provides rationale for deciding which system parameters (i. e. J -couplings, relaxation rates, reaction rate constants) have to be optimized in order to achieve higher signal enhancement for a substrate of interest in SABRE experiments.

Nuclear spin hyperpolarization is a rapidly growing field of Nuclear Magnetic Resonance (NMR). Presently, a number of hyperpolarization techniques are able to enhance the NMR sensitivity by several orders of magnitude in solid, liquid and gaseous samples.^{1–5} One of the most recent hyperpolarization techniques is Signal Amplification By Reversible Exchange (SABRE).^{6–10} In the SABRE effect, signal enhancement is endowed by a reversible association of parahydrogen (nuclear spin isomer of the hydrogen molecule with spin $I = 0$) and a to-be-polarized substrate with a metal complex, allowing the transfer of nuclear spin order from parahydrogen to the substrate.

SABRE is a physicochemical phenomenon which depends on both the magnetic resonance properties of the system (J -couplings, spin relaxation and/or decoherence times, etc.) and its chemical parameters (reactant concentrations, reaction rate constants, etc.). The nuclear spin polarization transfer is operative during the quantum-mechanical spin evolution in a coupled

multi-spin system, while chemical events are governed by the corresponding reaction rates. So far, only the physical nature of the SABRE phenomenon was accounted for properly, in particular, to describe the magnetic field dependence of the polarization transfer efficiency.^{11–13} Here we present a combined analysis of the chemical kinetics and the polarization transfer process, and derive a formula which describes the dependence of the enhancement factor in a SABRE experiment on the relevant concentrations as well as the exchange and relaxation rates. The derived expression explains well the results of published SABRE studies.

SABRE is typically observed for N-containing heterocycles, such as pyridine, nicotinamide, etc. (referred to below as “substrate”) when a metal complex (referred to below as “catalyst”) is used to briefly bring hydrogen and substrate into contact with each other and to facilitate exchange with their free states in solution.

It was found by Cowley et al.⁷ and Appleby et al.⁸ that the substrate exchange rate for the $[\text{Ir}(\text{IMes})\text{S}_3\text{H}_2]^+$ complex (IMes = 1,3-bis(2,4,6-trimethylphenyl)imidazol-2-ylidene, S = pyridine, pyridazine, or phthalazine)—thus far, the best SABRE catalyst—is independent of the substrate and hydrogen concentrations in solution. At the same time, the hydrogen exchange rate was found to be dependent on the solution composition: an increase in hydrogen concentration and a decrease in substrate concentration increases the hydrogen exchange rate.⁸ These results can be explained by assuming that (i) substrate substitution in the complex is a dissociative process (typically referred to in organic chemistry textbooks as $\text{S}_{\text{N}}1$ reaction), while (ii) hydrogen substitution is an associative process (referred to as $\text{S}_{\text{N}}2$ reaction) which requires formation of the intermediate species $\text{C}_1 = [\text{Ir}(\text{L})\text{S}_2\text{H}_2]^+$ (Figure 1). Indeed, owing to the chemical equilibrium between C (where $\text{C} = [\text{Ir}(\text{L})\text{S}_3\text{H}_2]^+$), S and C_1 , the concentration of C_1 can be expressed as $k_{\text{S}}^{\text{d}}[\text{C}]/k_{\text{S}}^{\text{a}}[\text{S}]$, where k_{S}^{d} and k_{S}^{a} are the substrate dissociation and association rate constants, respectively. According to the associative substitution mechanism for the hydrogen exchange (Figure 1b), one can find that the rate of hydrogen exchange (W_{H_2}) is indeed inversely proportional to the substrate

^a International Tomography Center, 3A Institutskaya st., Novosibirsk 630090, Russia
E-mail: danila.barskiy@tomo.nsc.ru; andrey.pravdivtsev@tomo.nsc.ru

^b Novosibirsk State University, 2 Pirogova st., Novosibirsk 630090, Russia

[‡] Electronic Supplementary Information (ESI) available. See DOI: 10.1039/b000000x/

[‡] Present address: Department of Radiology and Radiological Sciences, Institute of Imaging Science, Vanderbilt University, 1161 21st Avenue South, Medical Center North, AA-1105, Nashville, TN 37232-2310, USA.

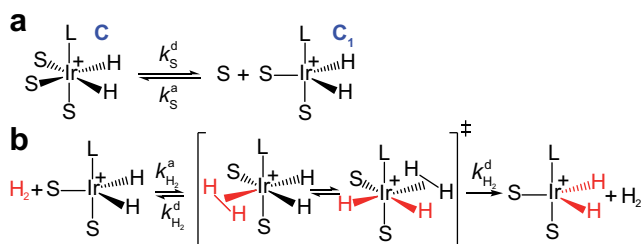


Fig. 1 Ligand exchange pathways for $[\text{Ir}(\text{L})\text{S}_3\text{H}_2]^+$ complexes (e. g., $\text{L}=1,3\text{-bis}(2,4,6\text{-trimethylphenyl})\text{imidazol-2-ylidene}$, $\text{S}=\text{pyridine}$): a) dissociative substrate exchange ($\text{S}_{\text{N}}1$), b) associative hydrogen exchange ($\text{S}_{\text{N}}2$).

concentration and is directly proportional to the hydrogen concentration:

$$W_{\text{H}_2} = \frac{k_{\text{H}_2}^{\text{a}}}{2} \left(\frac{k_{\text{S}}^{\text{d}}[\text{C}]}{k_{\text{S}}^{\text{a}}[\text{S}]} \right) [\text{H}_2] = \frac{k_{\text{H}_2}}{[\text{S}]} [\text{C}][\text{H}_2] = k'_{\text{H}_2} [\text{C}][\text{H}_2] \quad (1)$$

Further details on eq. (1) can be found in Electronic Supplementary Information (ESI†). The proposed scheme is in agreement with the fact that electron-rich 18-electron complexes do not have binding sites for association, whereas after dissociation of one of the ligands a 16-electron trigonal bipyramid is formed, which can undergo subsequent associative substitution.¹⁴ It should be pointed out that possible involvement of dihydrogen-dihydride intermediate $[\text{Ir}(\text{H}_2)(\text{H})_2(\text{L})(\text{S})_2]^+$ (Figure 1b) in the hydrogen exchange pathway was predicted by DFT calculations.⁷

To explain a polarization transfer mechanism in SABRE, we will use as an example the simplest spin system which is sufficient for the purpose, that is, the $\text{AA}'\text{B}$ -type three spin system. The spins AA' represent the strongly coupled Ir-HH hydride protons of the Ir-complex, while a single proton B of the substrate is coupled either strongly or weakly to the AA' protons depending on the applied magnetic field (Figure 2). It has been shown that coherent polarization transfer in SABRE is efficient at low magnetic fields, at the regions of Level Anti-Crossings (LACs).¹⁵ In the $\text{AA}'\text{B}$ -type system all three protons become strongly coupled and the energy levels of the two states $|\text{S}\alpha\rangle$ and $|\text{T}_+\beta\rangle$ approach each other but do not cross (due to the difference in AB and $\text{A}'\text{B}$ spin-spin couplings, Figure 2b). The initially overpopulated state $|\text{S}\alpha\rangle$ and the initially underpopulated state $|\text{T}_+\beta\rangle$ are mixed at such a LAC, and spin order is transferred from Ir-HH to the substrate. However, one should note that at high magnetic fields the SABRE mechanism is different: polarization transfer is incoherent, i.e., it occurs due to cross-relaxation in such a three-spin system.¹⁶

Let us introduce quantities $[\text{C}^*]$ and $[\text{S}^*]$ as concentrations of hyperpolarized species, for the complex and the free substrate molecule, respectively. These concentrations are determined as an imbalance between concentrations of molecules in the corresponding spin states: $[\text{C}^*] = [\text{C}_{|\text{S}\alpha\rangle}] - \frac{1}{3}([\text{C}_{|\text{T}_+\beta\rangle}] + [\text{C}_{|\text{T}_0\rangle}] + [\text{C}_{|\text{T}_-\beta\rangle}])$, $[\text{S}^*] = [\text{S}_{|\beta\rangle}] - [\text{S}_{|\alpha\rangle}]$, where the subset of states $\{\text{S}, \text{T}_+, \text{T}_0, \text{T}_-\}$ corresponds to the hydride protons and the subset $\{\alpha, \beta\}$ corresponds to the substrate proton. That is, $[\text{C}^*]$ corresponds to the imbalance between the concentrations of the singlet and the triplet states of Ir-HH in the complex; $[\text{S}^*]$ gives the “concentra-

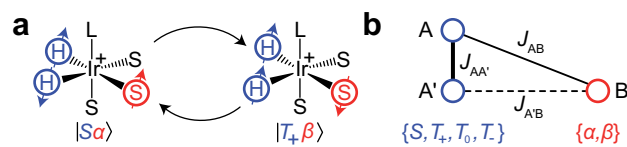


Fig. 2 a) Coherent SABRE polarization process in complex C between the spin states $|\text{S}\alpha\rangle$ and $|\text{T}_+\beta\rangle$. b) Schematic representation of complex C as an $\text{AA}'\text{B}$ spin system. Spins A and A' are strongly coupled at any field, thus, their states can be represented using the singlet-triplet basis. The state of spin B can be represented using the Zeeman states for a spin 1/2.

tion” of the net spin polarization of the substrate.

This description is convenient because one can show that the imbalance of the hydrogen isomer concentrations, $[\text{H}_2] = [\text{H}_2](4x_p - 1)/3$ (where x_p is the fraction of parahydrogen and $[\text{H}_2]$ is the hydrogen concentration in solution), is converted directly to the imbalance of complex states $[\text{C}^*]$ and, subsequently, to the imbalance of substrate states $[\text{S}^*]$ (see ESI†).

Let us now incorporate the exchange kinetics and polarization transfer into a common set of kinetic equations. In spite of the fact that polarization transfer in low-field SABRE experiments is a coherent process governed by the nuclear spin Hamiltonian, all spin coherences in the ensemble of complexes C are quickly washed out after the start of parahydrogen bubbling because the events of complex formation and dissociation are distributed in time. Consequently, the SABRE-derived polarization build-up is mainly determined by accumulation of populations during the chemical exchange and therefore can be treated using a set of chemical kinetics equations (Figure 3a).

Thereby, the polarization build-up starts with the formation of hyperpolarized species C^* (stage I in Figure 3a), which decays with the relaxation rate constant $R_{\text{C}} = 1/T_1^{\text{C}}$ (stage II) or takes part in the exchange process with the substrate with the above mentioned exchange rate constants k_{S}^{d} and k_{S}^{a} (stage III). The hyperpolarized substrate concentration $[\text{S}^*]$ decays with a rate constant $R_{\text{S}} = 1/T_1^{\text{S}}$ (stage IV, here we completely neglect the thermal polarization of S and C). Formation of C^* is magnetic field independent, while the subsequent processes—formation of the hyperpolarized substrate—depend on the NMR parameters of the system, e. g., on the magnetic field strength and J -coupling topology. In order to take this dependence into consideration, let us

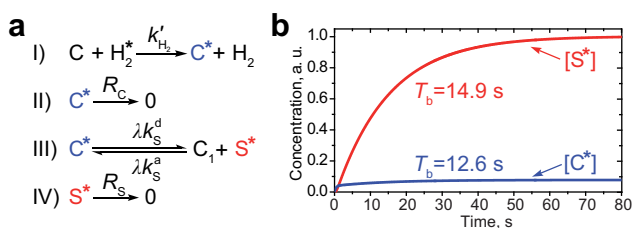


Fig. 3 a) Kinetic scheme describing the build-up of low-field SABRE-derived polarization. b) Calculated build-up curves for the hyperpolarized complex (C^* , blue line) and the substrate (S^* , red line). Parameters used in the calculations: $\lambda = 0.17$, $k_{\text{S}}^{\text{d}} = 10 \text{ s}^{-1}$, $R_{\text{C}} = 1/1.1 \text{ s}^{-1}$, $R_{\text{S}} = 1/27.5 \text{ s}^{-1}$, $[\text{C}] = 5 \text{ mM}$, $[\text{S}] = 90 \text{ mM}$.

introduce a factor of polarization transfer efficiency, λ . When polarization transfer is not efficient (i. e., λ is small), S^* is not produced in the polarization transfer stage III in Figure 3a. The analytical expression for the factor λ and its dependence on the magnetic field and rate constants is discussed in the text below.

Using the proposed kinetic model we found that the actual NMR signal enhancement factor, $|\epsilon|$, provided by SABRE is given by the following formula:

$$|\epsilon| = \eta \frac{[S^*]}{[S]} = \eta \left(\frac{4x_p - 1}{3} \right) \frac{[C][H_2]}{[S]^2} \frac{\lambda k_S^d k_{H_2}}{R_S(\lambda k_S^d + R_C) + R_C \lambda k_S^d \frac{[C]}{[S]}} \quad (2)$$

where $\eta = 0.5/P_{th} = kT/\gamma\hbar B_0$ is the maximal theoretical enhancement factor (for details of derivation see ESI†). It is readily seen that the signal enhancement (and the actual polarization, $P = \epsilon P_{th}$) is a combination of the above mentioned relaxation rates, R_C and R_S , and kinetic parameters, k_S^d and k_{H_2} . It is worth mentioning that in our kinetic scheme it is not important what kind of nuclei are polarized (e. g. 1H or ^{15}N) and what kind of polarization transfer mechanism is operative (e. g., the conventional coherent low-field SABRE mechanism⁶ or the high-field mechanism¹⁶ based on cross-relaxation): the peculiarities of a specific transfer mechanism are incorporated in the relaxation parameters R_C and R_S and in the factor λ . These parameters can be treated as external parameters for our model.

Several important consequences can be derived from analyzing equation (2). First, the signal enhancement is predicted to be directly proportional to the catalyst concentration for low $[C]$, and to be independent of the catalyst concentration for high $[C]/[S]$ ratios (i. e., when $R_S(\lambda k_S^d + R_C) \ll R_C \lambda k_S^d [C]/[S]$). The proportionality predicted for low $[C]$ follows from the fact that the complex C is the key molecule, in which polarization transfer takes place: the higher its concentration is, the higher is $[C^*]$. However, when $[C]$ is too high it brings about the fast relaxation of the substrate polarization, since generally $R_C \gg R_S$. Second, when $[C]/[S]$ is low (the substrate is present in large excess), the enhancement factor is proportional to the inverse square of the substrate concentration, because the formation of the intermediate C_1 responsible for the hydrogen exchange is suppressed and its concentration is low. In this case, polarization depends on the combination of the relaxation rates for the free and bound substrate and the dissociation rate constant. Third, when $[C]/[S]$ is high, the enhancement factor is inversely proportional to the substrate concentration and depends predominantly on the relaxation rate of the bound substrate.

The kinetic scheme shown in Figure 3a is also useful for analysis of the build-up rate of the SABRE-derived polarization. In general, starting from the same kinetic arguments, it can be shown that the effective substrate relaxation rate is given by $R_{eff} = (R_S + R_C[C]/[S])/(1 + [C]/[S])$ (see ESI†). This relaxation rate governs the substrate polarization build-up rate ($T_b = 1/R_{eff}$) and thus, we are able to evaluate T_b by substituting specific numbers into the above expression. By running additional measurements, we have found that at a high magnetic field (16.4 T, corresponding to the 700 MHz 1H NMR frequency) the average re-

laxation time of the protons of free pyridine used as the substrate is ~ 27.5 s (hence, $R_S \sim 0.036$ s $^{-1}$); for the protons of pyridine bound to the Ir-complex the average T_1 is about 3.6 s as measured by the inversion-recovery for protons of the non-exchanging axial pyridine ligand (hence, $R_C \sim 0.28$ s $^{-1}$). The T_1 time of pyridine is expected not to depend on the magnetic field strength, since conditions of the extreme narrowing regime apply and all protons in the coupled spin network have very similar relaxation rates.¹⁷ However, for pyridine ligand in the complex the relaxation time is expected to decrease when conditions of strong coupling with the hydride protons are fulfilled, i. e., at the LAC region. Hence, it is reasonable to assume $R_C \sim 0.9$ s $^{-1}$ (as for the hydride protons at high field) at 6 mT, which is a typical field for running low-field SABRE experiments. Taken this together, one can calculate the build-up time to be $T_b^{LF} \sim 12.2$ s for low-field SABRE and $T_b^{HF} \sim 20.3$ s for high-field SABRE. These values correlate well with the results published earlier.^{16,18} A more accurate analysis for low-field SABRE (based on the numerical simulation of the full kinetic scheme) gives the build-up time of 12.6 s for $[C^*]$ and 14.9 s for $[S^*]$ (Figure 3b). It is thus seen that the simplified evaluation for the build-up time is in a good agreement with these values.

We have analyzed the literature data and found that formula (2) explains well the trends observed in other studies (Figure 4). For example, it is seen that the signal enhancement is higher for lower substrate concentrations for both 1H and ^{15}N nuclei of the substrates;^{8,9} indeed, polarization as high as 10% was obtained only for low (~ 4 mM) substrate concentrations.¹⁹ However, substrate-to-metal ratio cannot be less than 3 because the active catalyst $[\text{Ir}(\text{L})(\text{S})_3(\text{H})_2]^+$ cannot be formed from the precursor (e. g. $[\text{IrCl}(\text{COD})(\text{IMes})]$) until 3 substrate molecules per Ir center are available as ligands. If the initial amount of substrate is low, then during bubbling with hydrogen one would expect the formation of Ir dimers²⁰ or other non-active species²¹ in solution. Therefore, the expected optimal substrate-to-metal ratio is ~ 3 . Formula (2) also explains the linear dependence of the SABRE enhancement on the catalyst concentration;^{7,22} however, $[C]$ values higher than 10 mM are usually limited by precursor

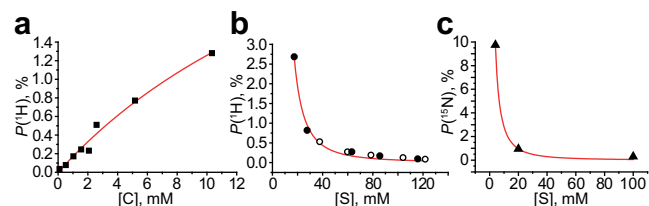


Fig. 4 a) 1H polarization dependence on the catalyst concentration (pyridine concentration is the same for all data points, $[S] = 103$ mM), data from ref. [7]; b) 1H polarization dependence on the substrate concentration, filled circles show data for pyridazine, empty circles show data for phthalazine (catalyst concentration was the same but was not specified by the authors), data from ref. [8]; c) ^{15}N polarization dependence on the substrate concentration (catalyst concentration $[C] = 0.2$ mM was the same for all data points); data from ref. [9]. The data sets shown were chosen because they provide polarization dependence on $[C]$ or $[S]$ concentration, with other parameters kept constant (see Figure S7 in ESI† for fitting details).

solubility. One may anticipate deviations from formula (2) when a strongly binding co-substrate is used along with polarizing substrates in micro- or nanomolar concentrations. In such a case, concentration of the intermediate species C_1 and the hydrogen exchange constant are independent of $[S]$ (see ESI†); therefore the signal enhancement should be independent of $[S]$, and the NMR signal of the polarized substrate should linearly depend on its concentration. This was indeed observed experimentally.²³

It is also seen from our model that the signal enhancement should be directly proportional to the rate of parahydrogen supply ($k_{H_2}[H_2^*]$). This expectation is confirmed by experiments in which the gas pressure and the parahydrogen flow rate were varied.^{9,24} This result means that much higher enhancements are expected if one could increase parahydrogen concentration in solution. While this may have seemed intuitive beforehand, we now provide a theoretical basis for why it should be so.

It is important to emphasize that although the parameter λ describing the spin mixing efficiency in SABRE complexes can be granted as an external parameter for our model, we can provide reasonable estimates for it. This can be done for both models of polarization transfer, which are currently being discussed: (i) coherent polarization transfer and (ii) cross-relaxation. For coherent polarization transfer, we derived the following expression:

$$\lambda_{\text{coh}} = \frac{\sin^2(2\theta)}{(k_S^d/\omega)^2 + 1} \quad (3)$$

where $\omega^2 = (\omega_A - \omega_B - 2\pi J_{AA'})^2 + \omega_{\text{LAC}}^2$, $\omega_k = (1 + \delta_k)\gamma_k B$, γ_k is the gyromagnetic ratio and δ_k is the chemical shift of nucleus k , $\omega_{\text{LAC}} = 2\pi|J_{AB} - J_{A'B}|/\sqrt{2}$ is a LAC angular frequency for a three-spin system and $\tan(2\theta) = \omega_{\text{LAC}}/(\omega_A - \omega_B - 2\pi J_{AA'})$ (for details see ESI†). At the center of the LAC region $\sin^2(2\theta) = 1$ and the parameter λ_{coh} has a sharp feature at the magnetic field corresponding to LAC and is close to zero otherwise. In the case of cross-relaxation, λ takes the form

$$\lambda_{\text{incoh}} = \frac{k_S^d(\sqrt{R_A} + \sqrt{R_B})^2}{(k_S^d + R_A)(k_S^d + R_B)} \quad (4)$$

where R_B and R_A are substrate and hydrides relaxation rates in the complex (see ESI† for derivation). Thus, we are able to take a quantitative account for the finite dissociation rate and describe the spin mixing efficiency. One clearly sees that for efficient hyperpolarization in the case of coherent transfer the rate of polarization transfer (ω_{LAC}) should be higher than k_S^d . For incoherent polarization transfer the condition $k_S^d = \sqrt{R_A R_B}$ provides the maximal transfer efficiency. However, one should bear in mind that too low k_S^d values in addition result in lower $[S^*]$ concentrations; thus, a compromise has to be found to ensure a high spin mixing efficiency and a sufficiently high dissociation rate.

Interestingly, the simple expression (3) can account for the so-called “quantum Zeno effect”.²⁵ Frequent substrate association-dissociation events act as quantum-mechanical “measurements” on the nuclear spin system and do not allow the system to evolve from the initial state, $|\alpha\rangle$, to the other state, $|\beta\rangle$, at the LAC. The functional dependence of λ on k_S^d is such that if we increase both k_S^d and k_S^a keeping their ratio (k_S^d/k_S^a) constant, the overall

enhancement decreases: indeed, repetitive “quantum measurements” on a spin system turn off the spin dynamics. Such an effect is absent in the cross-relaxation case (4), i. e., it is operative only in the case of true coherent quantum-mechanical spin evolution. A more detailed explanation of such behavior is given in ESI†; a rigorous theoretical analysis based on a quantitative spin dynamics simulation (taking into account the exact nature of spin dynamics and exchange kinetics) can confirm the presence of the quantum Zeno effect in SABRE experiments under multiple exchange events.²⁶ It is interesting to note that our model gives the maximal polarization as 50% ($\eta = 0.5/P_{\text{th}}$) for the substrate in low-field SABRE. In the case of incoherent polarization transfer the maximum achievable polarization depends on the cross-relaxation rate and the relaxation rate in the free substrate and the complex.

Summarizing all the results, one can see that the key parameters of the system which should be optimized are the relaxation rates (especially, R_C) and not the dissociation rate constants. Indeed, k_S^d is already on the order of 10 s^{-1} ,⁷ while the optimal value derived from the simple analysis as $k_S^d = \omega_{\text{LAC}}$ should be $\sim 4.5 \text{ s}^{-1}$ (for $J_{AB} - J_{A'B} = 1 \text{ Hz}$). As it was recently shown, there is a direct correlation between the substrate exchange rate and the π -accepting ability of the NHC ligands.²⁷ This observation together with the results presented here paves the way for prediction of the structure of more efficient catalysts for SABRE. One way to reduce the relaxation rate in the complex is to use deuterated ligands and substrates, which reduces the efficiency of the dipole-dipole relaxation mechanism in solution. It was shown by Fekete et al. that the deuteration of the NHC ligand indeed significantly increases polarization obtained by SABRE.²⁸ Another strategy is to increase the difference, $J_{AB} - J_{A'B}$, in J -couplings between the hydride and substrate nuclei: consequently, λ will still be large even at higher k_S^d . The J -coupling increase along with the prolongation of T_1^C and T_1^S explains the much higher enhancements observed for ^{15}N nuclei compared to ^1H nuclei of the substrates.¹⁹

To conclude, we have derived the formula that describes the dependence of the signal enhancement on the relevant parameters, such as concentrations of the catalyst, parahydrogen and substrate, J -couplings, relaxation rates and reaction rate constants for SABRE experiments. Although our formula is relatively simple, it is in a good agreement with the data published so far. Furthermore, based on its analysis we can formulate practical recommendations on how to design an optimal chemical system for SABRE: (i) the substrate-to-catalyst ratio should be as low as possible as long as C (e. g., $[\text{Ir}(\text{L})\text{S}_3\text{H}_2]^+$) remains the main catalyst form in solution, meaning that the optimal substrate-to-metal loading is ~ 3 (for lower ratios the formation of non-active species is expected); (ii) for low-field SABRE the substrate dissociation rate constant should be on the order of the spin mixing frequency at a LAC, $k_S^d = \omega_{\text{LAC}}$, while for high-field SABRE k_S^d should be as high as possible; (iii) relaxation sink in the complex C should be kept low, which can be achieved either by deuteration of the ligands or by using ligands carrying as few magnetic nuclei as possible; (iv) parahydrogen concentration in solution should be increased, either by using proper solvent, high pressure or by

an efficient gas-liquid mixing technology. We anticipate that the analysis presented here will be useful for optimization of experimental conditions in SABRE for the development of new NMR and MRI applications.

DAB, KVK and IVK thank RFBR grants (14-03-00374-a, 14-03-31239-mol-a and 14-03-93183 MCX_a) for support in conducting NMR experiments. ANP and KLI thank the Russian Science Foundation (grant No. 14-13-01053) for support in spin dynamics calculations.

References

- J. H. Ardenkjær-Larsen, B. Fridlund, A. Gram, G. Hansson, L. Hansson, M. H. Lerche, R. Servin, M. Thaning and K. Golman, *Proc. Nat. Acad. Sci.*, 2003, **100**, 10158–10163.
- P. Nikolaou, B. M. Goodson and E. Y. Chekmenev, *Chem. Eur. J.*, 2015, **21**, 3156–3166.
- B. M. Goodson, *J. Magn. Reson.*, 2002, **155**, 157–216.
- J. Natterer and J. Bargon, *Prog. Nucl. Magn. Reson. Spectrosc.*, 1997, **31**, 293–315.
- S. B. Duckett and R. E. Mewis, *Acc. Chem. Res.*, 2012, **45**, 1247–1257.
- R. W. Adams, J. A. Aguilar, K. D. Atkinson, M. J. Cowley, P. I. Elliott, S. B. Duckett, G. G. Green, I. G. Khazal, J. Lopez-Serrano and D. C. Williamson, *Science*, 2009, **323**, 1708–1711.
- M. J. Cowley, R. W. Adams, K. D. Atkinson, M. C. R. Cockett, S. B. Duckett, G. G. R. Green, J. A. B. Lohman, R. Kerssebaum, D. Kilgour and R. E. Mewis, *J. Am. Chem. Soc.*, 2011, **133**, 6134–6137.
- K. M. Appleby, R. E. Mewis, A. M. Olaru, G. G. Green, I. J. Fairlamb and S. B. Duckett, *Chem. Sci.*, 2015, **6**, 3981–3993.
- M. L. Truong, T. Theis, A. M. Coffey, R. V. Shchepin, K. W. Waddell, F. Shi, B. M. Goodson, W. S. Warren and E. Y. Chekmenev, *J. Phys. Chem. C*, 2015, **119**, 8786–8797.
- V. V. Zhivonitko, I. V. Skovpin and I. V. Koptuyug, *Chem. Commun.*, 2015, **51**, 2506–2509.
- R. W. Adams, S. B. Duckett, R. A. Green, D. C. Williamson and G. G. Green, *J. Chem. Phys.*, 2009, **131**, 194505.
- A. N. Pravdivtsev, A. V. Yurkovskaya, H.-M. Vieth, K. L. Ivanov and R. Kaptein, *ChemPhysChem*, 2013, **14**, 3327–3331.
- A. N. Pravdivtsev, K. L. Ivanov, A. V. Yurkovskaya, P. A. Petrov, H.-H. Limbach, R. Kaptein and H.-M. Vieth, *J. Magn. Reson.*, 2015, **261**, 73–82.
- C. H. Langford and H. B. Gray, *Ligand substitution processes*, WA Benjamin, Inc., 1966.
- K. L. Ivanov, A. N. Pravdivtsev, A. V. Yurkovskaya, H.-M. Vieth and R. Kaptein, *Prog. Nucl. Magn. Reson. Spectrosc.*, 2014, **81**, 1–36.
- D. A. Barskiy, K. V. Kovtunov, I. V. Koptuyug, P. He, K. A. Groome, Q. A. Best, F. Shi, B. M. Goodson, R. V. Shchepin, A. M. Coffey, K. W. Waddell and E. Y. Chekmenev, *J. Am. Chem. Soc.*, 2014, **136**, 3322–3325.
- K. Ivanov, A. Yurkovskaya and H.-M. Vieth, *J. Chem. Phys.*, 2008, **129**, 234513.
- D. A. Barskiy, K. V. Kovtunov, I. V. Koptuyug, P. He, K. A. Groome, Q. A. Best, F. Shi, B. M. Goodson, R. V. Shchepin, M. L. Truong, A. M. Coffey, K. W. Waddell and E. Y. Chekmenev, *ChemPhysChem*, 2014, **15**, 4100–4107.
- T. Theis, M. L. Truong, A. M. Coffey, R. V. Shchepin, K. W. Waddell, F. Shi, B. M. Goodson, W. S. Warren and E. Y. Chekmenev, *J. Am. Chem. Soc.*, 2015, **137**, 1404–1407.
- M. L. Truong, F. Shi, P. He, B. Yuan, K. N. Plunkett, A. M. Coffey, R. V. Shchepin, D. A. Barskiy, K. V. Kovtunov, I. V. Koptuyug, K. W. Waddell, B. M. Goodson and E. Y. Chekmenev, *J. Phys. Chem. B*, 2014, **118**, 13882–13889.
- B. J. van Weerdenburg, A. H. Engwerda, N. Eshuis, A. Longo, D. Banerjee, M. Tessari, C. F. Guerra, F. P. Rutjes, F. M. Bickelhaupt and M. C. Feiters, *Chem. Eur. J.*, 2015, **21**, 10482–10489.
- K. D. Atkinson, M. J. Cowley, P. I. Elliott, S. B. Duckett, G. G. Green, J. Lopez-Serrano and A. C. Whitwood, *J. Am. Chem. Soc.*, 2009, **131**, 13362–13368.
- N. Eshuis, B. J. van Weerdenburg, M. C. Feiters, F. P. Rutjes, S. S. Wijmenga and M. Tessari, *Angew. Chem. Int. Ed.*, 2015, **54**, 1481–1484.
- R. V. Shchepin, M. L. Truong, T. Theis, A. M. Coffey, F. Shi, K. W. Waddell, W. S. Warren, B. M. Goodson and E. Y. Chekmenev, *J. Phys. Chem. Lett.*, 2015, **6**, 1961–1967.
- W. M. Itano, D. J. Heinzen, J. Bollinger and D. Wineland, *Phys. Rev. A*, 1990, **41**, 2295.
- S. Knecht *et al.*, *in preparation*.
- B. J. van Weerdenburg, N. Eshuis, M. Tessari, F. P. Rutjes and M. C. Feiters, *Dalton Trans.*, 2015, **44**, 15387–15390.
- M. Fekete, O. Bayfield, S. B. Duckett, S. Hart, R. E. Mewis, N. Pridmore, P. J. Rayner and A. Whitwood, *Inorg. Chem.*, 2013, **52**, 13453–13461.